ERDA/JPL 954471-77/3
Distribution Category UC-63
1978

Quarterly Progress Report No. 11
Covering the Period 1 August 1978 to 31 October 1978

NOVEL DUPLEX VAPOR-ELECTROCHEMICAL METHOD FOR SILICON SOLAR CELLS

By: V. Kapur, K. M. Sancier, A. Sanjurjo, S. Leach,
S. Westphal, R. Bartlett, and L. Nanis

Prepared for:

JET PROPULSION LABORATORY
California Institute of Technology
4800 Oak Grove Drive
Pasadena, California 91103

Attention: Dr. Ralph Lutwack
Spacecraft Power Station

Contract No. 954471 under NAS 7-100
SRI Project PYU 4980

(NASA-CR-158039) NOVEL DUPLEX VAPOR ELECTROCHEMICAL METHOD FOR SILICON SOLAR CELLS Quarterly Progress Report, 1 Aug. - 31 Oct. 1978 (SRI International Corp., Menlo Park, Calif.) 55 p HC A04/MF A01 CSCL 10A G3/44

N79-14537

Unclas
41044



SRI International
333 Ravenswood Avenue
Menlo Park, California 94025
(415) 326-6200
Cable: SRI INTL MNP
TWX: 910-373-1246



CONTENTS

LIST OF ILLUSTRATIONS iii
LIST OF TABLES iv
PREFACE v
SUMMARY vi

1. SiF_4-Na Reaction: Solid Na Feeding 1

Introduction 1

Experimental 2

Reaction Products: Solid Na Feed 4

2. Na_2SiF_6-Na Reaction: Thermite Reaction 6

Introduction 6

Experimental Results 7
Initial Confirmation 7
Reaction Parameters 7
Mechanism Studies 8
Scale-Up Studies 10
Design Improvement Studies 15

3. Silicon Separation: Leaching Studies 24

Introduction 24

Results 25

Discussion 28
Decrease in Hydrogen Evolution Rate in Solution 28
Decrease in Hydrogen Evolution Due to Aging in Air . . . 31

Conclusions 32

4. Silicon Separation: Melting Studies 34

Silicon Separation by Melting the Reaction Products 34
Purification of Silicon by Solidification 42

PRECEDING PAGE BLANK NOT FILMED

ILLUSTRATIONS

		Page
1	Reactor for the SiF_4-Na Reaction: Solid Na Feeding Technique	3
2	Reaction Product Obtained by the SiF_4-Na Reaction: Solid Feeding Technique	5
3	Experimental System to Study the Na_2SiF_6-Na Reaction	9
4	Reactor for the Na_2SiF_6-Na Reaction: Second Scale-up Experiment	14
5	Reaction Product of the Na_2SiF_6-Na Reaction: Second Scale-up Experiment	16
6	Reactor for the Na_2SiF_6-Na Reaction Design Improvement	18
7	Reaction Product from the Na_2SiF_6-Na Reaction	20
8	Hydrogen Evolved by Silicon Powder in Acid Fluoride Solution as a Function of Time	27
9	Hydrogen Evolved by Silicon Powder in Acid Fluoride Solution as a Function of Square Root of Time	29
10	Increasing Molten Silicon Contact Angle on Graphite with Increasing Contact Time in the Presence of NaF	35
11	Extraction of Impurities by Molten NaF in Contact with Molten Si	39
12	Calculated Change in the Equilibrium Mole Fraction of Various Components in the Gas Phase of the Si-NaF-Ar System with Total Pressure	41
13	Silicon Purification by Directional Solidification	46

TABLES

		Page
1	Emission Spectrographic Analysis of the Na_2SiF_6-Na Reaction Products. First Scale-up Experiment	12
2	Emission Spectrographic Analysis of the Na_2SiF_6-Na Reaction Product: Design Improvement	22
3	Emission Spectrographic Analysis of Impurities in Si and NaF Phases Obtained After Melting Metallurgical-Grade Si with Reagent-Grade NaF in a Graphite Crucible	38
4	Impurity Analysis of Silicon by SSMS	43
5	Segregation Coefficients for Various Impurities	44
6	Permissible Impurity Concentrations in Solar Cell Silicon	45

PREFACE

The JPL Low-Cost Silicon Solar Array Project is sponsored by the U. S. Department of Energy and forms part of the Solar Photovoltaic Conversion Program aimed at the development of low-cost solar arrays. This work was performed for the Jet Propulsion Laboratory, California Institute of Technology, by agreement between NASA and DOE.

This report was prepared as an account of work sponsored by the United States Government. Neither the United States nor the United States Department of Energy, nor any of their employees, nor any of their contractors, subcontractors, or their employees, makes any warranty, expressed or implied, or assumes any legal liability or responsibility for the accuracy, completeness, or usefulness of any information, apparatus, product or process disclosed, or represents that its use would not infringe privately owned rights.

SUMMARY

A simplified feed system for the Na used in the Na-SiF_4 reactor has been developed. Solid Na is added directly to the reaction zone, thus avoiding the handling of liquid Na.

The reduction of sodium fluosilicate with sodium metal has been proven to be an alternative path for the production of high purity silicon. Batches containing about 1 kg of silicon have been produced with a purity similar to the products obtained with the SiF_4-Na reaction.

During the leaching process to recover silicon from the products of the SiF_4-Na reaction, hydrogen is evolved. Kinetic studies indicate that the hydrogen evolution may be a diffusion-limited process. Mechanism studies are continuing; at present, it appears that small amounts of sodium are incorporated in the silicon, although the type of inclusion is uncertain. During leaching, the resulting local regions of high alkalinity could promote the oxidation of silicon.

Studies of silicon separation by the melting of the reaction product have been continued. Analyses have been made of the purification of the processes of melting and solidification. Reaction products from both the SiF_4-Na reaction and the Na_2SiF_6-Na reaction have been successfully separated by melting to yield silicon in bulk form.

1. SiF_4 REACTION: SOLID Na FEEDING

By: A. Sanjurjo, S. Westphal

Introduction

This section describes a new technique for feeding Na as a solid into the Na-SiF_4 reactor.

At SRI International, it has been demonstrated that when SiF_4 is put in contact with Na at temperatures above 150°C, a very rapid exothermic reaction takes place. The reaction can be made self-sustaining by the addition of discrete quantities of Na into a reactor maintained under a constant pressure of SiF_4. In our previous approach, drops of liquid Na at about 130°C were fed through a "shower head" injector in the top of the reactor into an atmosphere of SiF_4. When the Na drops reached the bottom of the reactor (maintained at temperatures above 250°C), reaction (1) occurred very rapidly.

$$SiF_4(g) + 4Na\ (\ell) = Si(c) + 4NaF\ (c/\ell) \qquad (1)$$

This technique requires a careful control of the Na temperature at the Na inlet. For example, if the Na temperature reaches 150°C, premature reaction takes place and the reaction products can plug the injector.

We have developed a simplified alternative technique in which Na is fed into the reactor as solid pieces. In this technique, the heat generated by the reaction is used to melt Na and to heat it to reacting temperature. To test this method, a new series of experiments have been carried out in the reactor used previously for the liquic Na feeding experiments, with modifications described as follows.

Experimental

In the solid feeding method, Na slices (ca. 6 mm thick, 6.3 cm. diam.) are loaded in a side arm of the reactor head, as shown in Figure 1. The side arm is lined with a polypropylene sheath to avoid contamination of the Na by the glass walls. The remainder of the reactor is operated the same as for the liquid Na feeding method.[1] Vacuum and SiF_4 lines are connected to the reactor by the central opening at the reactor head. The temperature of the SiF_4 is monitored by a thermocouple (TC).

The reactor has a double lining (Grafoil within Ni) that prevents contamination of the reaction product. A NaF bed keeps the reaction products from sticking to the bottom Ni cup. To start the reaction, external heat is provided to bring the initial piece of Na to the reacting temperature of about 150°C. Once the reaction has started, external heating can either be maintained or turned off. During the reaction, the slices of Na are pushed by a rod in the side arm until they drop into the reaction zone where they are heated. Depending on the size of the slice, the time required to heat the Na to reacting temperature ranges from a few seconds to a few minutes. The Na then reacts with the SiF_4 within a few seconds.

[1] Quarterly Progress Report No. 10

ORIGINAL PAGE
OF POOR QUALITY

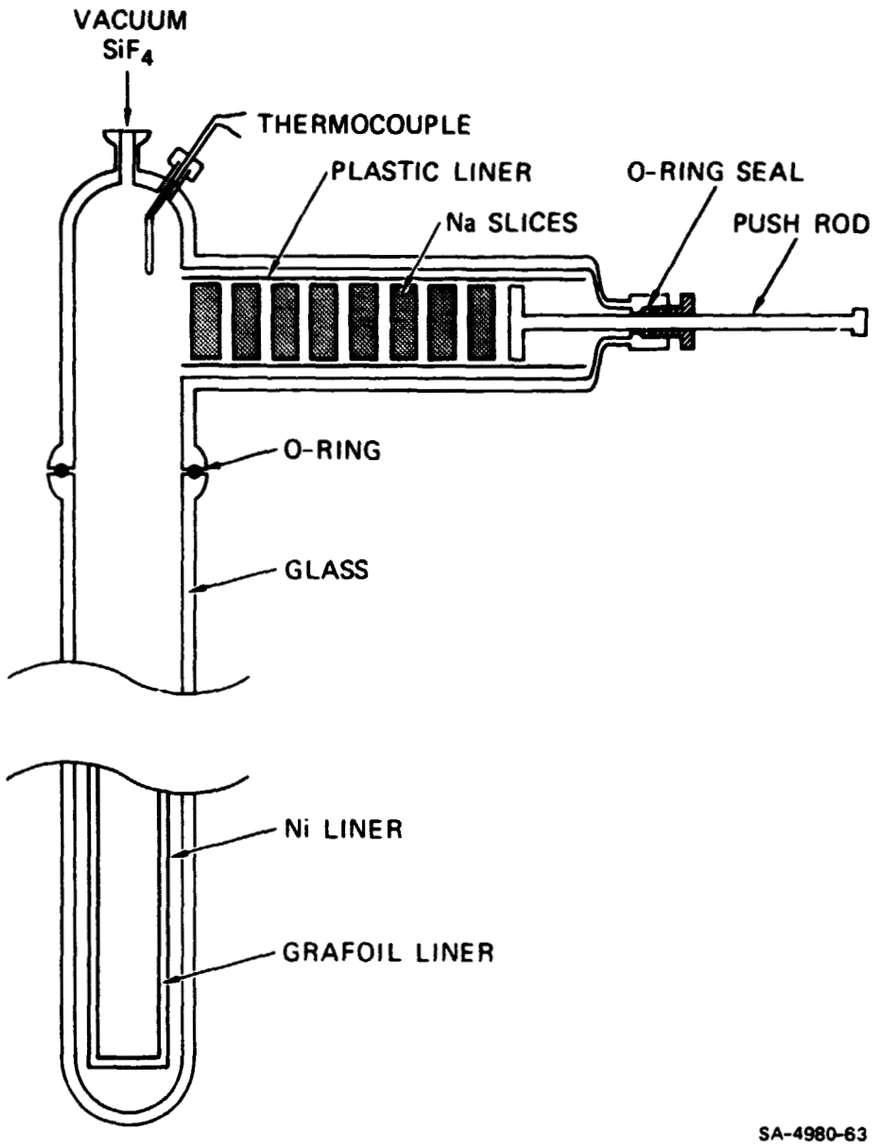


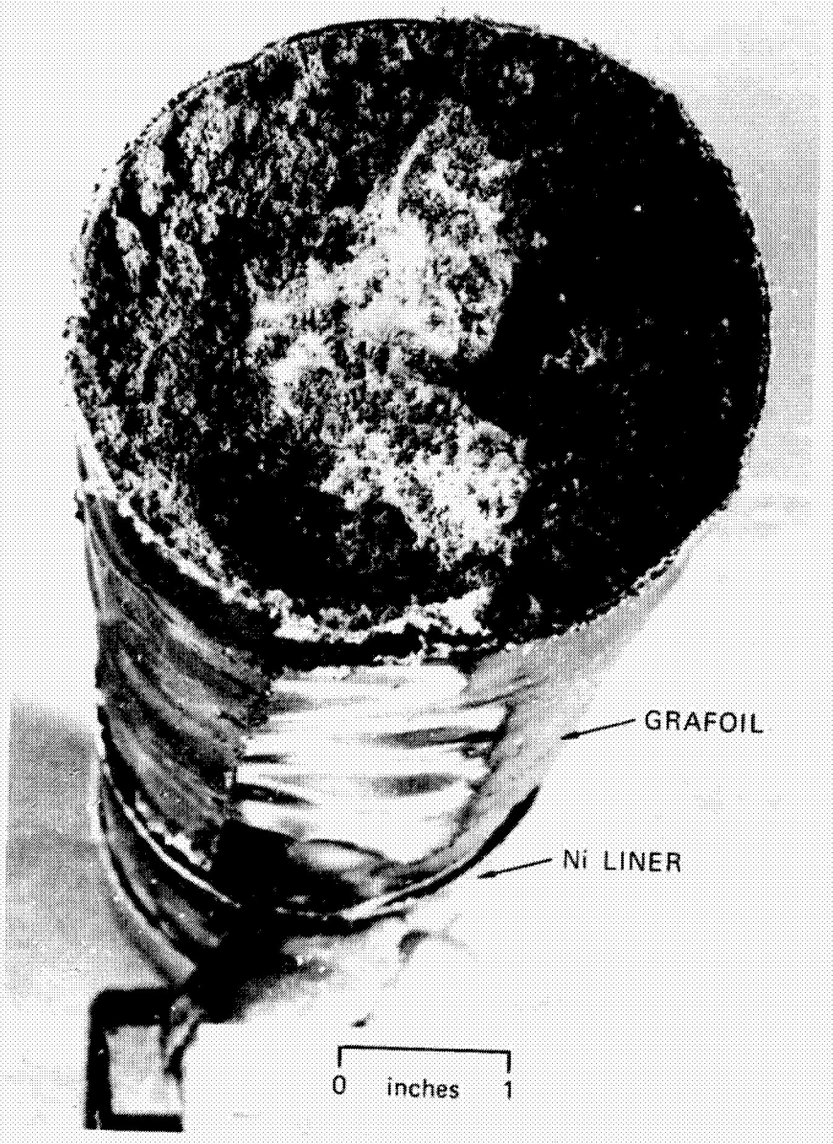
FIGURE 1 REACTOR FOR THE SiF_4-Na REACTION: SOLID Na FEEDING TECHNIQUE

Reaction Products: Solid Na Feed

As expected, the reaction products from the solid feeding method are very similar in composition and purity to those obtained by the liquid Na feeding method. X-ray analysis indicates the presence of Si, NaF, and some Na_2SiF_6. Emission spectrographic analysis indicates that the only element present at a detectable level is Ca, which is probably introduced by the Na reactant.

A notable difference in the two methods is the tendency of the reaction products obtained by the solid Na feeding to occupy the entire volume enclosed by the Grafoil liner, as shown in Figure 2.

ORIGINAL PAGE IS
OF POOR QUALITY



SA-4980-64

FIGURE 2 REACTION PRODUCT OBTAINED BY THE SiF_4-Na REACTION: SOLID FEEDING TECHNIQUE

2. Na_2SiF_6-Na REACTION: THERMITE REACTION

By: A. Sanjurjo, R. Bartlett, and S. Leach

Introduction

At SRI International we have demonstrated that high purity silicon can be produced by the sodium reduction of silicon tetrafluoride according to the highly exothermic (ΔH^o_{298} = -164 Kcal/mol) reaction:

$$SiF_4 \ (g) + 4 \ Na \ (l) = Si \ (c) + 4 \ NaF \ (c/l)^* \qquad (1)$$

We have also shown that SiF_4 gas can be generated by the thermal decomposition of sodium fluosilicate according to the reaction.

$$Na_2SiF_6 \ (c) = SiF_4 \ (g) + 2 \ NaF \ (c), \qquad (2)$$

which is endothermic (ΔH^o_{298} = + 40 Kcal/mol).

In the current procedure, these two reactions are operated independently, with the SiF_4 produced in a separate reaction (Eq. 2) being fed to the reduction reactor (Eq. 1). A more economic and energy-efficient procedure could be devised in which the heat liberated by the reduction reaction (1) is used to produce SiF_4 by the decomposition reaction (2); this could be accomplished by allowing both reactions to occur simultaneously in the same process unit operation. In such a process, silicon could be produced directly by the reaction between sodium and fluosilicate according to:

$$Na_2SiF_6 \ (c) + 4 \ Na \ (l) \rightarrow Si \ (c) + 6 \ NaF \ (c) \qquad (3)$$

Reaction (3) is thermodynamically favorable for the production of silicon with ΔH^o_{298} = - 124 Kcal/mol. From our experience with the kinetics of

*g = gas l = liquid c = crystal

reactions (1) and (2), we can estimate the temperature range at which the overall reaction (3) should be rapid. During previous research done at SRI International, it has been observed that reaction (1) occurs at SiF_4 pressures as low as 70 torr. In addition, we have observed that this level of pressure can be obtained from the decomposition of Na_2SiF_6 at approximately 550°C. Therefore, it was expected that reaction (3) would start at temperatures equal to or less than 550°C. During this quarter, we have studied the characteristics of reaction (3) and the reaction product obtained. For convenience we refer to this as the thermite process because of its similarity to other thermite metal reduction processes conducted in sealed vessels.

Experimental Results

Initial Confirmation

Direct reaction according to (3) was first verified experimentally on a small scale. A piece of Na (1 g) and a stoichiometric amount of Na_2SiF_6 powder were loaded in a nickel cup, which was then introduced into a glass reactor. The reactor was evacuated and then heated externally. At approximately 500°C, an almost instantaneous reaction took place, giving reaction products of similar characteristics to those obtained by the SiF_4-Na process (Eq. 1). X-ray analysis indicated the presence of Si, NaF, and Na_2SiF_6. The absence of H_2 evolution when the solid reaction products were added to dilute acid indicated that all of the Na had reacted.

Reaction Parameters

To gain more information about the characteristics of reaction (3), we built a new cylindrical (3 in. x 12 in.) stainless steel reactor in which both temperature and pressure could be measured. The reactor is

shown in Figure 3. The reactor was tightly closed by means of two flanges and a copper gasket. The top flange had two openings; one allowed the introduction of chromel alumel thermocouples (TC1, TC2) and the other was connected to a vacuum line. The reactor was inserted in a thermally insulated well containing an electrical heater at the bottom. This well was surrounded by sand as a safety measure in case of pressure release.

In this experiment, 10 g of Na, in 1-2 g pieces, was loaded with a stoichiometric amount of Na_2SiF_6 powder. The reactor was then evacuated and heated at the bottom until the reaction started. The following information was obtained from this experiment:

- The reaction initiated at approximately 520°C, as indicated by (TC1).
- The maximum measured temperature reached at the bottom of the reactor was approximately 1150°C.
- The reaction began at the bottom and then propagated toward the top at a rate of 4 cm/sec, as determined from the spacing between TC1 and TC2 and the time lag between starting reaction times at the thermocouple tips.
- The temperature increase at the top of the reactor caused by the reaction was from 335°C to 760°C as recorded by TC2.
- The pressure remained at vacuum level except at the very start of the reaction, when it rose rapidly to approximately 1.5 atm.

Mechanism Studies

Some insight into the mechanism by which reaction (3) takes place has been gained by experimentally demonstrating the presence of SiF_4 (g) as an intermediate. Sodium was loaded in a copper cylindrical cup

ORIGINAL PAGE IS
OF POOR QUALITY

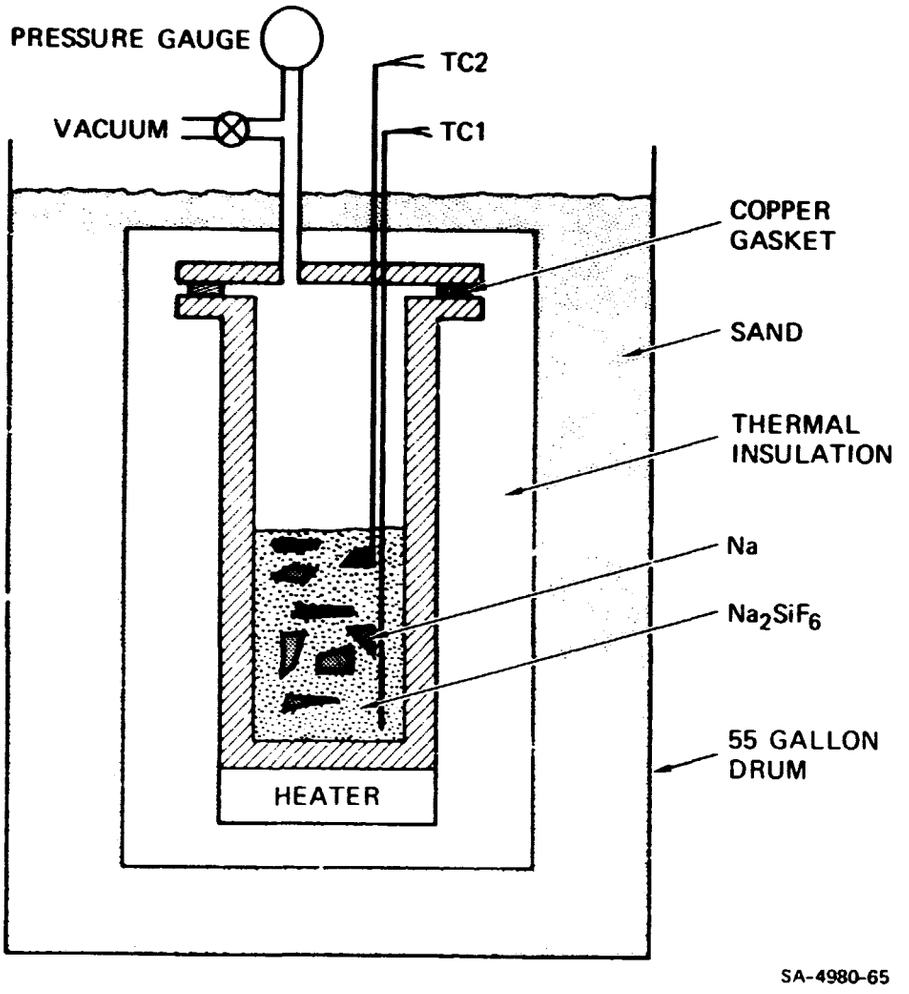


FIGURE 3 EXPERIMENTAL SYSTEM TO STUDY THE Na_2SiF_6-Na REACTION

(1.5 in dia. x 4 in.) which was then placed in an Al_2O_3 tube (2.5 in. i.d.). Sodium fluosilicate was added in the annular space between the copper and the alumina. Thus, the reactants were separately loaded in two concentric compartments, divided laterally by a copper wall. This geometry allowed for an efficient heat transfer from the inner (Na) compartment to the outer (Na_2SiF_6) compartment and allowed for easy vapor transport to the sodium. This system was placed in the stainless steel reactor Figure (3), which was then evacuated and backfilled with argon. The reactor was heated to 500°C and reaction took place in the inside compartment, as indicated by an increase in temperature.

X-ray analysis indicates that after the reaction, the inner compartment (Na) contained Si and NaF and that the outer compartment contained NaF and Na_2SiF_6. From this information, we concluded that during the initial heating, some SiF_4 (g) is generated by Na_2SiF_6 decomposition. The SiF_4 (g) reaches the liquid Na and reacts with it to produce silicon according to reaction (1) and to liberate heat. As heat is released, Na_2SiF_6 is decomposed further, generating more SiF_4 (g). The process continues until one of the reactants has been depleted. The overall reaction (3) is very fast (order of seconds) for 10 g of Na. The pressure build-up is minimal (less than 3 atm) and is due partially to the thermal expansion of argon initially present at 1 atm.

Scale-Up Studies

Because of the promising results obtained with the thermite process (reaction 3), we performed scale-up experiments to evaluate reaction yield. Two scale-up experiments were performed with 100 g and 4.5 kg of Na, respectively. In the first scale-up experiment, approximately 100 g of Na in 2g to 5 g pieces and a stoichiometric amount of Na_2SiF_6 were loaded in a

cylindrical steel reactor (3 in. i.d. x 6 in.). The reactor was made out of low-carbon steel and both ends were closed by means of a threaded cap and plug. Sauereisen cement was used to make the reactor gas tight to prevent the escape of SiF_4 (g). The loaded reactor was placed inside the insulating chamber described in Figure 3; however, in this experiment, the entire surface of the reactor was heated by electrical heating elements.

After reaction, the reactor was cut open and examined. A sponge-like reaction product occupied most of the volume. X-ray analyses indicated the presence of Si, NaF, and some Na_2SiF_6. Unreacted Na was well below 5 percent by weight of the reaction product. The purity of the reaction product, as determined by emission spectroscopy, is shown in Table 1. The purity is good considering that the reactants were loaded directly in contact with the steel walls without any special precaution. The presence of Fe (175 ppm) and Ca (150 ppm) can be attributed to the experimental conditions. Iron contamination results from the direct contact of the products with the reactor walls and calcium is introduced by the reactants; Na contains 100-200 ppm Ca and Na_2SiF_6 contains up to 50 ppm Ca.

The second scale-up experiment had two main purposes:

- To scale-up the amount of reactants by a factor of 50.
- To test a reactor design in which the heat of reaction is used to self-propagate the reaction.

In the second scale-up experiment, 4.5 kg of Na and a 10% excess over the stoichiometric amount of Na_2SiF_6 were used. This amount of reactant should produce approximately 1.4 kg of Si. The Na was cut into cylindrical slices (2.5 in. dia. x 0.5 in.) of approximately 30 g each. To accommodate this amount of reactants, a large reactor was constructed of welded

Table 1

EMISSION SPECTROGRAPHIC ANALYSIS OF Na_2SiF_6-Na REACTION PRODUCT: FIRST SCALE-UP EXPERIMENT

Element	Amount (ppm by weight)
Si	High level
Na	Principal constituent
Al	8.
Fe	175.
Cu	< 4.
Ca	150.
Ti	6.
Ni	< 8.
B	< 30.
Zr	< 7.5
Ba	< 6
V	< 5
Cr	< 3.5
Mn	< 4.
P	< 4500.
Mg	< 6.
Ag	< 5.
Mo	< 3.5

low-carbon steel. The reactor is sketched in Figure 4. An opening on the top allows for a thermocouple well that contains three thermocouples--TCA, TCB and TCC. The thermocouple tips were spaced 20 cm apart to measure the temperature at different points inside the reactor; TCB and TCC measured the temperature in the lower two-thirds of the reactor occupied by reactants, and TCA measured the temperature in the empty space above.

To allow reaction (3) to be self-propagating and to avoid energy input for heating the reactor and contents to 500°C, an initiation section was provided at the bottom of the reactor with a section of smaller diameter (3 in.), as shown in Figure 4. This section can be heated easily to 500°C to start the reaction, using a propane-O_2 torch.

The reaction started naturally first at the bottom of the reactor where the temperature increased to 950°C. The intermediate thermocouple TCB recorded a temperature jump from room temperature to 430°C at a time 2.7 minutes later. The rate of reaction propagation (0.12 cm/sec) was much lower than that mentioned above in which preheating to 500°C produced a 4 cm/sec propagation speed. The temperature registered by TCA increased steadily from room temperature at the start of reaction to 400°C after 18 minutes.

After the reaction was completed, the reactor was opened by cutting off the top third. The top of the reactor contained a brown formation analogous to the reaction products obtained by the SiF_4-Na reaction, indicating that the reaction had propagated all the way to the top.

It was found that some Na (approximately 20%) had not reacted. We attribute this to two factors. First, some of the Na_2SiF_6 may have settled

ORIGINAL PAGE IS
OF POOR QUALITY

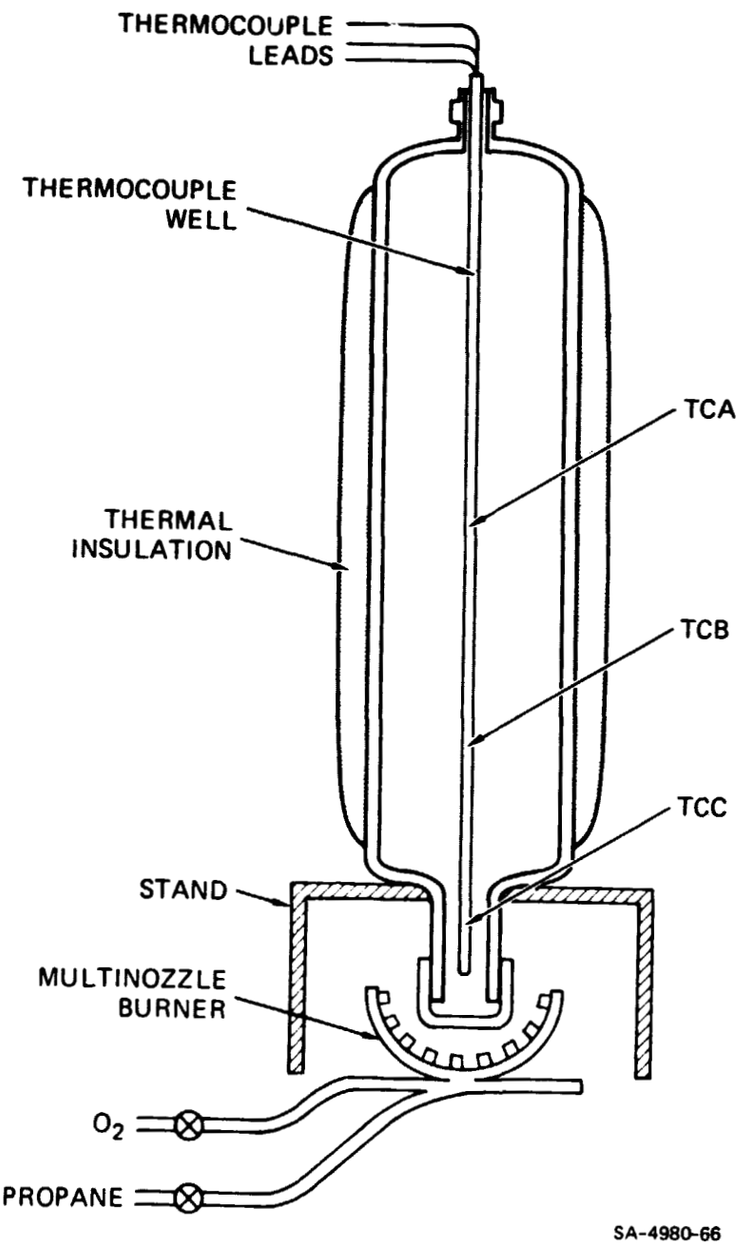


FIGURE 4 REACTOR FOR THE Na_2SiF_6-Na REACTION: SECOND SCALE-UP EXPERIMENT

toward the bottom during handling, causing segregation of the reactants. Also, the temperature reached at the top of the reactor was not high enough, because of insufficient internal heat liberated by the reaction itself.

In general, the reaction products are similar to those obtained earlier in the small-scale thermite experiments. One striking new feature, shown in Figure 5, consists of various "pockets" with numerous silicon needles (1-10 mm long and 0.1-1 mm wide).

Design Improvement Studies

The results of the mechanism and scale-up experiments showed that the thermite process has several desirable characteristics, including:

- Simplicity and ease of scale up
- Low cost reactants
- Surprisingly pure reaction products.

Therefore, a series of new experiments has been planned to refine both the technique and the design of the reactor used in this process.

The first experiment of this series had three main objectives:

(1) To decrease the amount of unreacted sodium

(2) To facilitate the removal of the reaction products

(3) To increase the purity of the reaction products.

Several possible approaches can be used to decrease the amount of unreacted sodium. First, the reactor could be made more adiabatic so that less heat is transferred to the environment. Second, the geometry of the reactor could be changed to favor a more rapid heat transfer through the reactants. Third, the reactants could be preheated so that the reaction-produced temperature wave would exceed the 500°C level. This final approach, together with a homogeneous premixing of reactants, was adopted for the first design improvement experiment.

ORIGINAL PAGE IS
OF POOR QUALITY

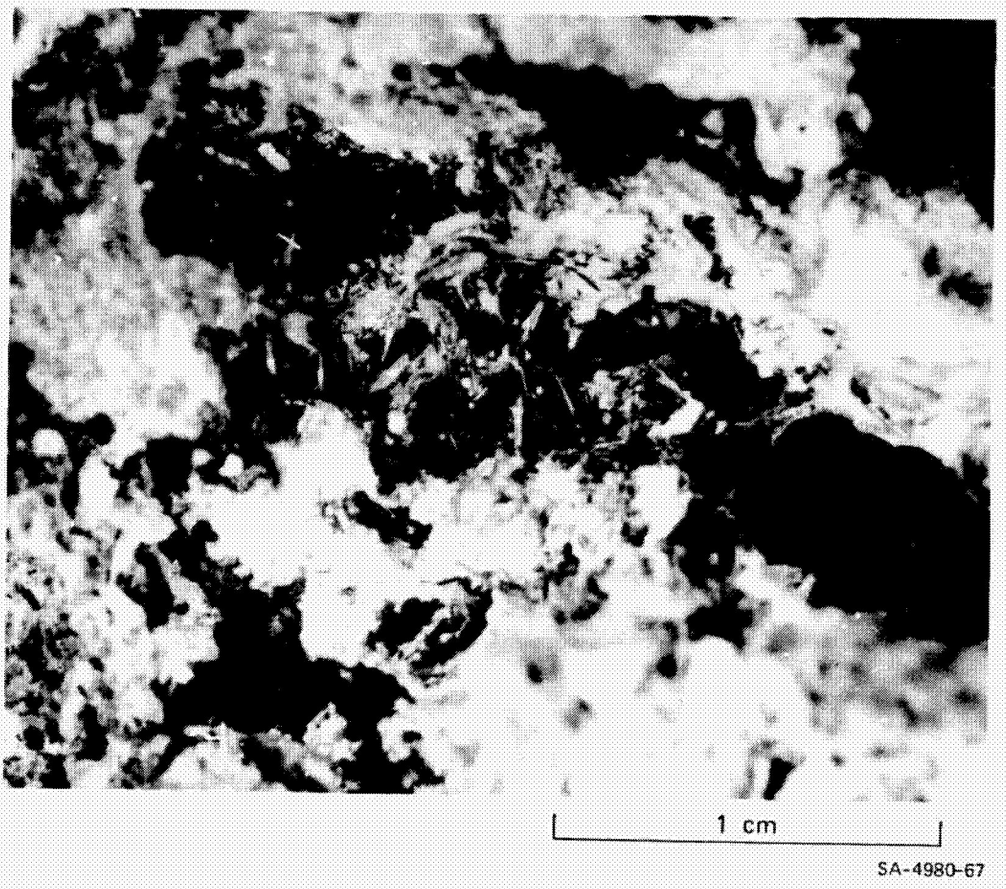


FIGURE 5 REACTION PRODUCT OF THE Na_2SiF_6-Na REACTION: SECOND SCALE-UP EXPERIMENT

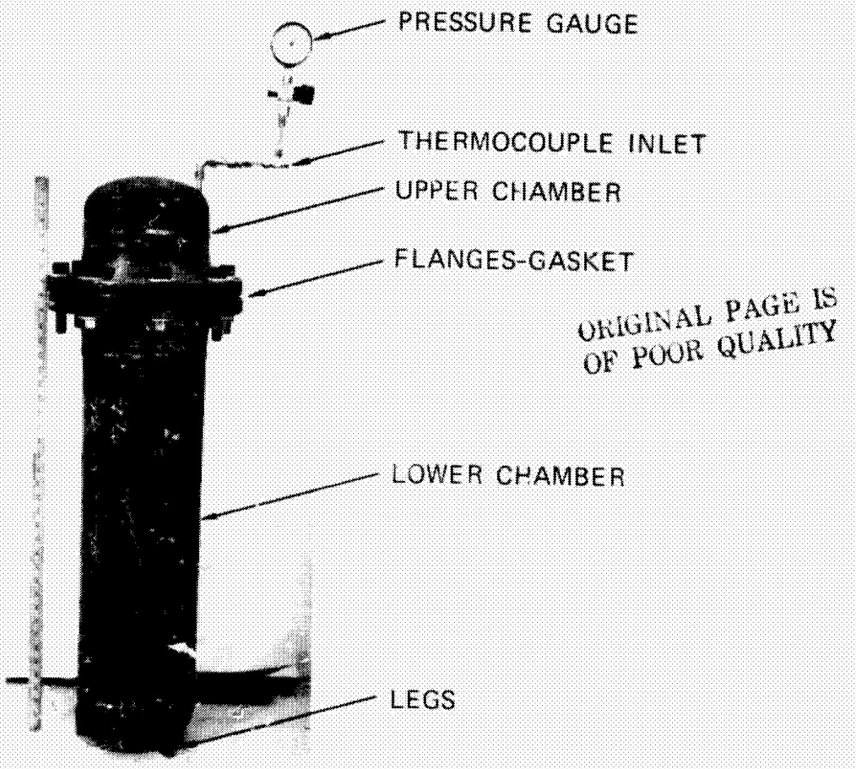
Thin-walled inner liners were used to increase the purity and to facilitate the removal of the reaction products. The liners provided a mechanical way to keep the reaction product from adhering to the reactor walls and reduced to a minimum the contamination of the reaction products by the reactor walls.

Reactor Design

Subsequent experiments were carried out in a cylindrical (8 in. i.d.x34 in.) low-carbon steel pipe (Schedule 80) reactor, shown in Figure 6. The reactor was made gas-tight by means of a flange-gasket system. Steel flanges and asbestos-graphite gaskets suitable for temperatures as high as 1000^{o}C were used. The upper and lower chambers of the reactor were each welded to flanges that could be bolted together.

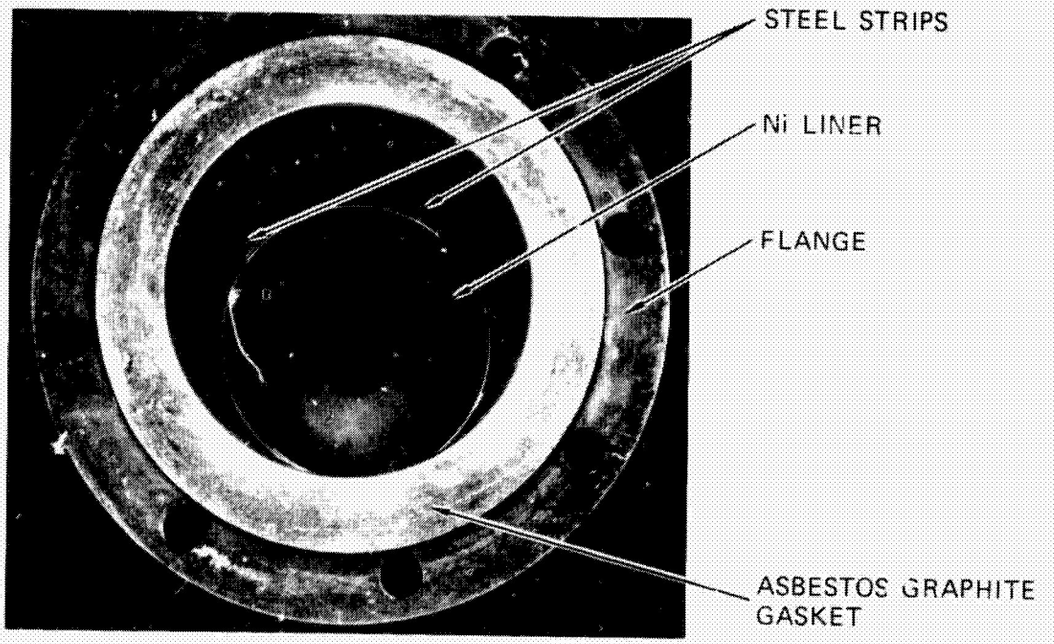
To facilitate the extraction of the reaction products, four symetrically located 1/4-in.-thick steel strips were welded along the length of the inner reactor walls. The purpose of these strips is to reduce the reactor's inner diameter with respect to the mouth of the flange. A sheet Ni liner 0.01 in. thick was fitted just against these strips, permitting easy in and out motion of the liner. Four symmetrically located holes were drilled on the upper part of the Ni liner to provide a handle hold for extracting the liner. In addition to the Ni liner, a Grafoil liner, 0.01 in. thick, separated the reaction products from the reactor walls. The main purpose of the Grafoil liner is to prevent contamination of the reaction products by the Ni liner.

The pressure was monitored by a gauge, PG, connected to the reactor by 3/8-in. stainless steel tubing. The temperature was monitored at three positions -- 10 cm, 40 cm, and 70 cm measured from the bottom of



LATERAL VIEW

ORIGINAL PAGE IS
OF POOR QUALITY



TOP VIEW OF LOWER CHAMBER

SA-4980-68

FIGURE 6 REACTOR FOR THE Na_2SiF_6-Na REACTION: DESIGN IMPROVEMENT

the reactor. The thermocouple wires were placed between the Ni liner and the reactor walls and were protected by a Ni sheath (0.005 in.).

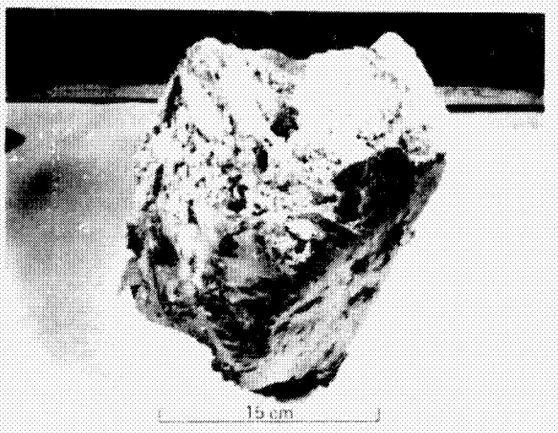
Reaction Experiment and Reaction Products

To preheat the system (reactor and reactants), a flame capable of heating a large area was necessary. A kerosene-compressed air torch was used for this purpose. The temperature of the system was first steadily increased to about 250°C during 1 hour. Because of the uneven pattern of the flame, large gradients (±50°C) developed along and, presumably, across the reactor. The fuel feeding rate was approximately 0.1 gallon of kerosene per minute. The feeding rate was then increased to 0.5 gallon per minute and the temperature rose steadily for 0.5 hour until it reached approximately 400°C, at which point the reaction started. The average temperature increased over 100°C in a matter of seconds. At this point, the recorded temperatures varied between 560°C and 800°C, depending on location. The reactor was kept at this temperature level for 20 minutes by the kerosene flame to ensure complete reaction. During this period the pressure inside the reactor was approximately 3 atm, which basically corresponds to the thermal expansion of the initial argon. The reactor was finally allowed to cool, whereupon pressure in the reactor dropped back to 1 atm.

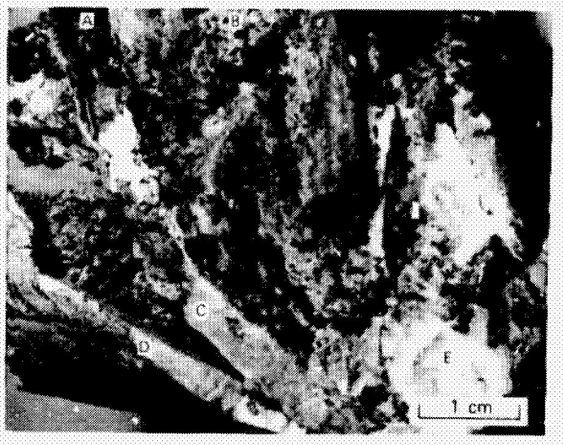
The reaction products consisted of a porous mass occupying the same volume as the initial reactants. Large masses (Figure 7a) of the reaction products were easily removed from the reactor without fragmentation, as shown in Figure 7. The Grafoil liner, although deformed and even broken in some places, survived well, as may be seen in the lower right part of Figure 7a.

Three visually different types of materials can be observed in the reaction products: grey crusts (Figure 7b; positions, A,B,C,), white

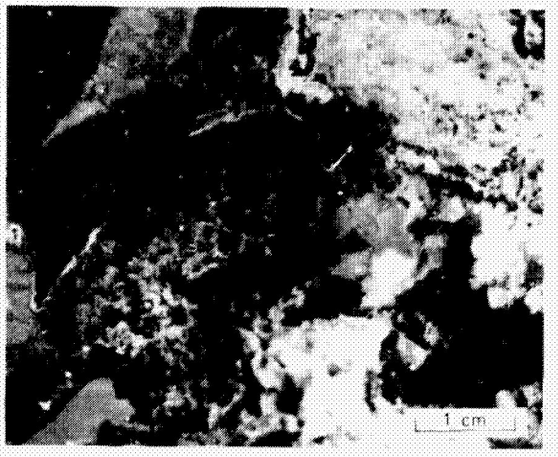
ORIGINAL PAGE IS
OF POOR QUALITY



(a) GENERAL VIEW OF A SAMPLE PIECE



(b) GENERAL MORPHOLOGY



(c) WHITE BUBBLY FORMATION



(d) HARD CONTINUOUS MATERIAL

SA-4980-69

FIGURE 7 REACTION PRODUCT FROM THE Na_2SiF_6-Na REACTION

bubbly formations (Figure 7b; position E), and a white hard continuous material (Figure 7b; position D). The grey crust seems to have formed along the outline of former Na solid blocks. The Na apparently melts out of the blocks to form reaction products (B,C,), leaving behind a void space (A). X-ray analyses indicate that the grey crust consists mostly of Si and NaF.

The white bubbly formation contains both NaF and Na_2SiF_6 (Figure 7c). Finally, the white hard and compact material located preferentially along the Grafoil liner (Figure 7d) is also a mixture of NaF and Na_2SiF_6, as determined by X-ray analysis.

Randomly selected samples of reaction products from different volumes of the materials identified in the previous section were analyzed for the presence of unreacted sodium. The procedure used was a direct titration of a known amount of reaction products with 0.1N HCl. This procedure was used only as a semi-quantitative indication of the amount of unreacted Na. The results obtained indicate that the weight percentage of unreacted sodium in the white materials (Figure 7b) is practically zero and is about 8 percent by weight of the reaction product in the grey crusts (Figure 7b; positions A,B,C,).

Purity of the Reaction Products

Because the grey crusts are the silicon-rich parts of the polyphase reaction products, more emphasis has been placed on their analyses than on the other materials identified. Four samples of grey crust were taken at random from different locations and one sample each was taken from the white bubbly material and from the white hard continuous material. Table 2 lists the impurity content of these samples as determined by emission spectrographic analysis. In addition, for comparison purposes,

Table 2

EMISSION SPECTROGRAPHIC ANALYSIS OF THE Na_2SiF_6-Na REACTION PRODUCT: DESIGN IMPROVEMENT (CONCENTRATION REPORTED IN PPM BY WEIGHT)

	Reactants		Reaction Products (Polyphase Mixture)							
			GREY CRUST				White Porous Material	White Compact Material	Unreacted Na_2SiF_6	Grafoil
Element	Na	Na_2SiF_6	a	b	c	d				
Al	< 2.5	20	8	20	20	15	20	25	25	50
Ca	10-100	35	150	70	100	150	70	70	40	200
Fe	< 7-35	< 7	20	15	15	7	< 7	15	7	20
Mg	17		< 6							6
Cu	4-8		< 4							< 4
Ba			< 6							< 6
Mn			< 4							< 4
Ti			< 6							< 6
Zr			< 7.5							< 7.5
V			< 5							< 5
Cr			< 3.5							< 3.5
Ag			< 5							< 5
Mo			< 3.5							< 20
P			< 4500							< 4500
B			< 30							< 30
Ni			< 8							< 8
Na	 Principal constituent in all samples									
Si	 High in all samples									*

*Major element, but would not be considered a "principal constituent."

Table 2 lists the impurity content of the unreacted Na_2SiF_6 powder, the impurity content of the reactants Na and Na_2SiF_6, and also of the Grafoil. The impurity content of the commercial Na varies within certain limits, which are listed for pertinent elements.

The only detectable impurities by emission spectrographic analyses in the reaction products were Al, Ca, and Fe. Most of the Al and some Ca may have been introduced from the industrial-grade Na_2SiF_6 used. Impurities in the sodium may be responsible for the introduction of the rest of the Ca and possibly the Fe. In future experiments, we will use reactants of greater purity so as to pinpoint the source of impurities that appear in the product. However, based on thermodynamic criteria and emission spectrographic analysis of silicon and sodium fluoride after their separation we know that essentially all of the Al and Ca are contained as fluorides in the NaF salt.

3. SILICON SEPARATION: LEACHING STUDIES

By: K. M. Sancier and V. Kapur

Introduction

We have continued to study the leaching process for recovering silicon from the reaction products of the SiF_4-Na reaction. The objectives of the current work are (1) to understand the mechanism by which the silicon yield is decreased by silicon oxidation during the leaching process and (2) to make recommendations for minimizing this silicon oxidation.

We previously reported[1] that the oxidation of silicon during leaching is accompanied by the evolution of hydrogen gas according to

$$Si + 4\,H_2O \rightarrow Si(OH)_4 + 2\,H_2 \qquad (4)$$

The hydrogen evolution rate was found to be proportional to the fluoride ion concentration. The fluoride ion is present because of the solubility of NaF and Na_2SiF_6 in the leaching solution. We concluded that the extent of the oxidation could be decreased and the silicon recovery could be increased by carrying out the leaching process as rapidly as possible. In this way, the silicon is exposed only briefly to high fluoride ion concentrations, especially because the NaF is more soluble than Na_2SiF_6. The action of fluoride ions in promoting silicon oxidation is believed to involve removal of a protective silicon dioxide coating on the silicon grains, thus permitting reaction (4) to proceed rapidly.

[1] Quarterly Progress Report No. 10.

In the current quarterly period, we examined the kinetics of the hydrogen evolution that occurs when leached silicon alone is in contact with an acid fluoride solution. The results can be interpreted by a hydrogen evolution process that is diffusion limited, together with a mechanism of silicon oxidation that entails the promoting action of metallic sodium incorporated in the silicon.

Results

In continuing work, we attempted to obtain kinetic information on the hydrogen evolution rate as a function of the fluoride ion concentration over a more detailed range than had previously been studied.[1] The silicon used in these studies was recovered by leaching the products of Run 2.[1] These reaction products were composed of a mixture from several batches that were produced by the SiF_4-Na reaction, and the storage time that any of these batches were exposed to air was less than 30 days prior to the time of leaching of Run 2. Hydrogen evolution was measured for the silicon powder in a solution containing 1.2 N H_2SO_4 and NaF at various concentrations, according to the procedure described previously in Quarterly Progress Report No. 10.

We discovered that the silicon had become much less active under the same experimental condition used a few months previously (i.e., 0.6 N NaF and 1.2 N H_2SO_4). The decrease in activity appeared to be related to the time that elapsed between the initial silicon recovery by leaching and the measurement of the hydrogen evolution rate. This effect of the age of the silicon on the hydrogen evolved is shown in Figure 8, for samples of the silicon tested at 7, 94, and 154 days after recovery from leaching. Also shown (right-hand ordinate) is the loss of silicon calculated from the hydrogen evolved according to the stoichiometry of reaction (4). The

results indicate that the rate of hydrogen evolution decreased in two different ways: (1) during a measurement, for example, at a given "age," and (2) with the age of the silicon.

To determine whether the decrease in hydrogen evolution rate was caused by a build up of a protective silicon dioxide layer, we treated a sample of the silicon 122 days old with 25 weight percent hydrofluoric acid for 1 hour. The purpose of this treatment was to remove any surface silica that may have formed with aging. For the HF-treated sample, the hydrogen evolution versus time relationship was about the same as for 154-day-old silicon (Figure 8). This result suggests that a buildup of a protective silica layer is not a determining factor in the long-term aging effect.

In other experiments, we determined that the hydrogen evolution was negligible for 70-day-old silicon in 1.2 N H_2SO_4 solutions containing either 0.12 or 0.25 N NaF. However, this silicon was very reactive when introduced into a concentrated alkaline solution (1.0 N NaOH) with an initial hydrogen evolution rate of 170 cc/min, a very rapid rate compared with 0.2 cc/min, which is the fastest rate for the results in Figure 8.

The hydrogen evolution characteristics of a different sample of silicon powder were examined. This silicon was prepared by leaching a reaction product (Run 9) that had been stored in air for 70 days after its preparation by the SiF_4-Na reaction. The time dependence curve for the hydrogen evolution was of similar shape to the 94-day silicon shown in Figure 8, but the hydrogen evolved at any given time as about one-third less. Although composition of various reaction products may differ greatly among batches, one potentially significant difference is the content of unreacted sodium, as discussed below. The sodium contents of the

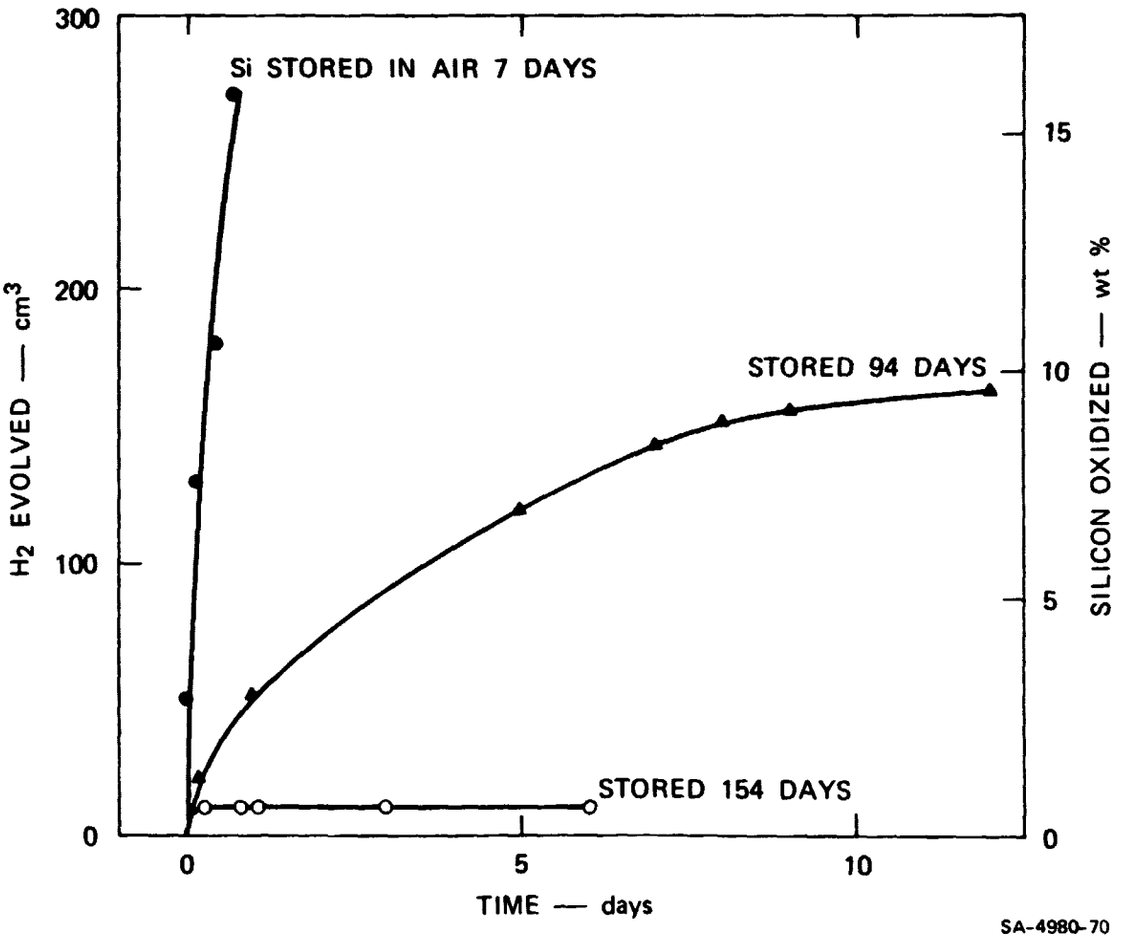


FIGURE 8 HYDROGEN EVOLVED BY SILICON POWDER IN ACID FLUORIDE SOLUTION AS A FUNCTION OF TIME

1.0g Si in 100 ml solution 0.60N NaF and 1.2N H_2SO_4.

reaction products used in Runs 2 and 9 were 16 and 4 weight percent, respectively.

The silicon from Run 9 was heated in a high temperature mass spectrometer to determine whether metallic sodium was present in the leached silicon. We observed evidence of sodium atoms from a peak at 23 mass units, and the assignment was confirmed by the characteristic appearance potential of 4.5 eV. The sodium peak first appeared for a sample temperature of 300°C, and the intensity increased substantially at 400°C. Metallic sodium would be expected to be detected at lower temperature, such as 200°C. We also observed evidence of SiF_4 evolution when the silicon was heated to 370°C. The mass peaks due to SiF_4^+ and SiF_3^+ were strong, and the presence of two isotopic species of SiF_3^+ confirmed the assignment. The SiF_4 probably arises from Na_2SiF_6 in the silicon that has not been removed by leaching. Incidentally, observed sodium atoms could not have been produced by thermal decomposition of Na_2SiF_6.*

Discussion

Two phenomena associated with hydrogen evolution from silicon are recognized. The first is the decrease in the evolution rate while the silicon is in the acid fluoride solution. The second is the decrease in the evolution rate that results from storing the silicon in air. These two phenomena will be discussed separately.

Decrease in Hydrogen Evolution Rate in Solution

The curve shapes in Figure 8 suggest that a diffusion limited process may be controlling the rate of hydrogen evolution. To test this hypothesis, the data in Figure 8 were replotted according to the parabolic rate law (hydrogen volume versus square root of time) as shown in Figure 9. The

*Results of an unpublished study by K. Lau at SRI.

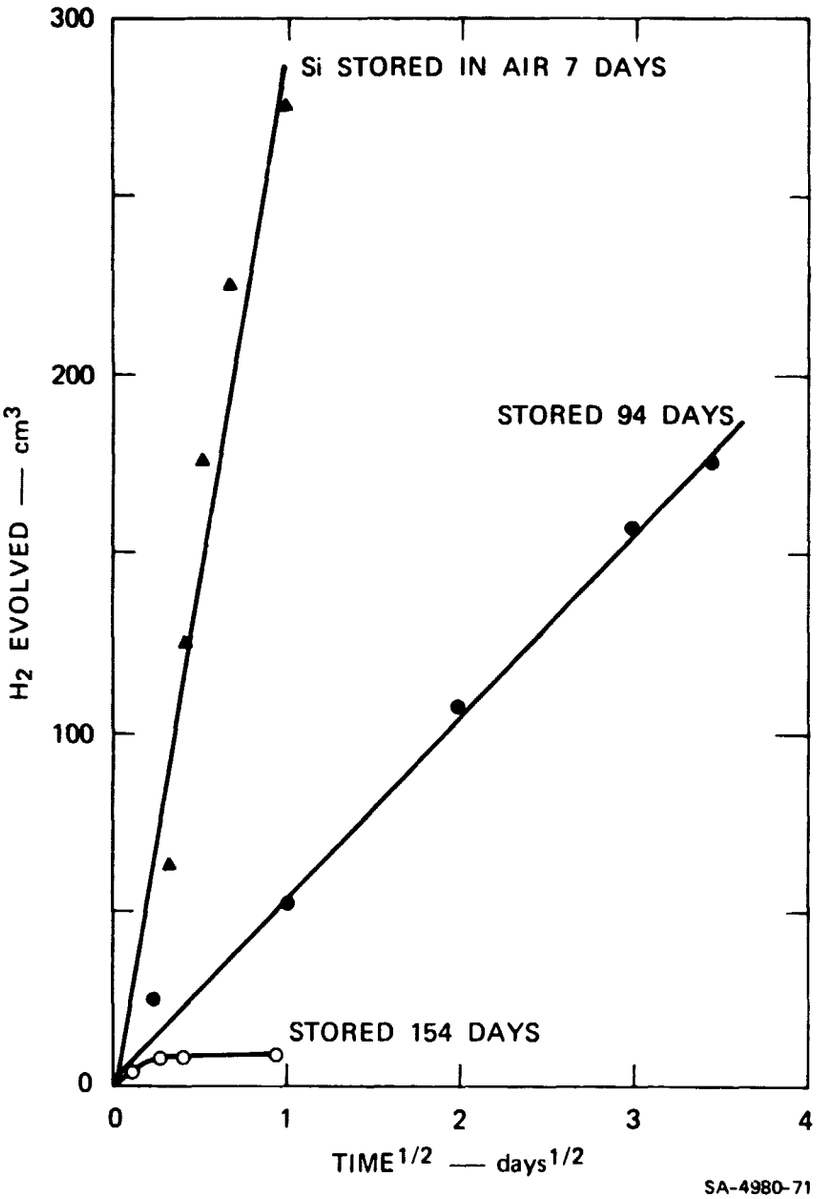


FIGURE 9 HYDROGEN EVOLVED BY SILICON POWDER IN ACID FLUORIDE SOLUTION AS A FUNCTION OF SQUARE ROOT OF TIME

Data from Figure 8.

linear curves obtained in Figure 10 for the 7- and 94-day-old samples generally support a diffusion limited mechanism. The curve for the 154-day-old sample does not fit as well. However, because the activity of the silicon in the latter sample had decreased to a very low level, some other mechanism may be active.

To account for the hydrogen evolution, we propose that our samples of silicon contain metallic sodium, which acts as a promoter for reaction (4). Sodium is known to be present in high concentrations (0.75 and 0.20 weight percent in the silicon of Runs 2 and 9, respectively) as indicated by emission spectrographic (ES) analysis. The presence of metallic sodium was demonstrated by the high temperature mass spectrometric measurement. The fact that sodium remained in the silicon after extensive leaching suggests that the sodium is in the bulk of silicon where it is not readily accessible to the leach solution.

The sodium in the silicon could not account for the amount of hydrogen produced, even assuming all the sodium reacts as metal. For example, for Run 2, if all the sodium were in the metallic state, the maximum amount of hydrogen would be 3.9 cc, compared with the 270 cc actually collected during several hours for the 7-day-old silicon (Figure 8). Therefore, we conclude that the sodium serves as a promoter for reaction (4). Metallic sodium in silicon could promote the oxidation of silicon by providing a local, highly alkaline environment in which silicon is known to be rapidly oxidized with resulting hydrogen evolution.

The diffusion limited process leading to hydrogen evolution must depend on the diffusion of a reactant, probably acidified water, along grain boundaries or through a microporous structure in silicon that results from the "etching" out of sodium. As the etching proceeds, the reaction path

becomes longer, and the rate of the reaction tends to become diffusion limited. The degree of alkalinity that develops locally in the pores and the rate of hydrogen evolution would depend on the amount of sodium in silicon and the path length for diffusion of the acid solution. The transport of reactants is also affected by the stirring produced by hydrogen gas motion in the pores. The shape of the hydrogen evolution curve of the 154-day-old silicon (Figure 8) suggests that almost all the metallic sodium had been oxidized before the test.

The sodium metal in the silicon could be present in several forms: interstitially dissolved in the silicon, microdroplets at grain boundaries, or in a microporous structure of the silicon, or as a silicide. The sodium silicides, $NaSi_2$ and NaSi, have been reported as stable compounds that dissociate only when heated to 420°C in vacuum.[2,3]

Decrease in Hydrogen Evolution Due to Aging in Air

The results in Figure 9 show that a sample of silicon produces less hydrogen the longer the sample is aged in air. Two mechanisms were considered to account for this decreased activity upon aging the silicon. According to the first mechanism, a protective layer of silicon dioxide builds up on the silicon surface with time, and the reactivity of the silicon becomes less as the silicon dioxide layer becomes thicker or denser. However, this mechanism was shown not to be significant by the experiment in which an HF-treatment was used to remove the surface oxide layer and the silicon activity did not increase.

The second mechanism proposed is related to the decrease in hydrogen evolution rate discussed in the previous section. As the silicon is stored in air, the sodium in the silicon is gradually oxidized by oxygen and/or water vapor. The microporous structure that results from this oxidation

[1] "Constitution of Binary Alloys," M. Hansen and K. Anderko, eds., (McGraw Hill Book Co., Inc. 1958).

[2] Ibid, First Supplement, 1965.

then increases the diffusion path required for the acid fluoride solution to react with the remaining sodium. Accordingly, the transport rate of reactants may be expected to decrease with the age of the silicon, as shown in Figure 8.

Conclusions

Silicon is oxidized by the acid fluoride leaching solution, as indicated by the hydrogen evolved. We propose that this oxidation is promoted by the oxidation of metallic sodium in the silicon structure, which in turn produces high local alkalinity that promotes silicon oxidation. The hydrogen evolution rate appears to be a diffusion rate limited process. The diffusion limited process may be accounted for by formation of a microporous structure in the silicon that results from the sodium being "etched" from the silicon. Silicon aged in air and then placed in an acid fluoride solution has lower activity for hydrogen evolution. Aging silicon in air results in lower activity for hydrogen evolution when the aged silicon is subsequently introduced into an acid fluoride solution. This lower activity is caused partly by the sodium having been oxidized and partly by the microporous structure in the silicon that results in a diffusion limited reaction. The role of the acid fluoride solution in the oxidation of silicon is to remove the protective silicon dioxide layer, but this removal process is apparently much more efficient in concentrated alkaline solution.

The practical consequence of these results is that losses of silicon by oxidation can be decreased by (1) leaching the reaction product as soon as possible after it is produced, and (2) leaching as rapidly as possible. Moreover, it may be possible to avoid the sodium problem by performing the

SiF_4-Na reaction under experimental conditions where sodium metal is not present in the silicon, for example, at higher temperatures. The possibility should be considered that if sodium is present in the silicon, the yield of silicon from the SiF_4-Na reaction may be decreased by prolonged storage in air either of the reaction products before leaching or of the silicon recovered by leaching. That is, the sodium may promote the oxidation of silicon by air.

4. SILICON SEPARATION: MELTING STUDIES

By: V. Kapur, R. Bartlett

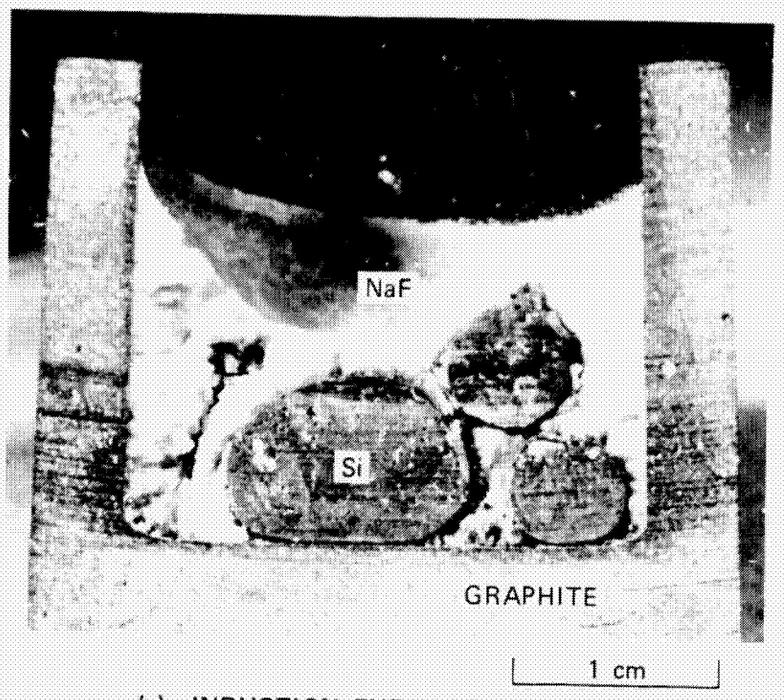
Silicon Separation by Melting of Reaction Products

Studies of silicon separation by the melting of the as-produced mixture of NaF and Si from the SiF_4-Na reaction were continued. As reported in Quarterly Report No. 10, heating the reaction products above 1410°C (mp of Si) in a graphite crucible agglomerates liquid silicon, which is more dense than NaF and settles to the bottom of the crucible. Liquid sodium fluoride, which melts at 993°C, is immiscible with silicon and usually wets graphite in the presence of liquid silicon. However, in some experiments molten silicon has spread on the crucible even in the presence of molten NaF. The two photographs in Figure 10 show molten silicon at different contact angles on the crucible. At present, we do not know the cause of variable spreading. It may be due to impurity surfactant effects or conversion of the graphite wall to SiC. However, we have observed SiC on the crucible wall with silicon that did not wet the crucible bottom surface.

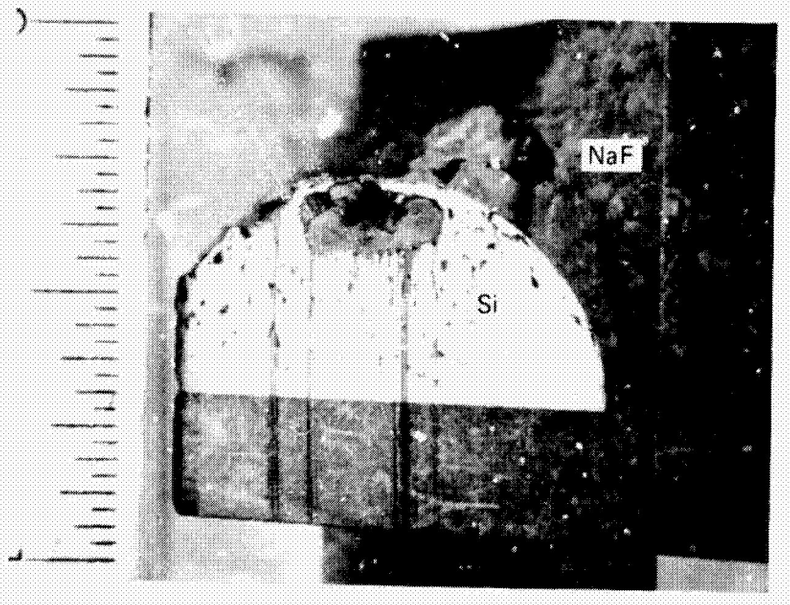
Analysis of a silicon obtained by melt separation at SRI showed that nickel (400 ppm) was the major impurity. The heavy nickel contamination in this particular sample was caused by the nickel liner used in the SiF_4-Na reduction reactor.

The NaF phase obtained after melting the reaction products was analyzed by energy dispersive x-ray fluorescence in a scanning electron microscope; the analysis qualitatively indicated the presence of some metallic impurities in the NaF phase. Any impurities in adjacent silicon

ORIGINAL PAGE IS
OF POOR QUALITY



(a) INDUCTION FURNACE (5 minutes)



(b) RESISTANCE FURNACE (20 minutes)

SA-4980-72

FIGURE 10 INCREASING MOLTEN SILICON CONTACT ANGLE ON GRAPHITE WITH INCREASING CONTACT TIME IN THE PRESENCE OF NaF(l)

were undetectable by this method. Prompted by this observation, we investigated the effect of molten NaF as a solvent for extracting impurities from molten silicon. Molten sodium fluoride is a very good metallurgical flux and it dissolves most metallic oxides and fluorides. To examine this behavior, we melted a mixture of metallurgical-grade silicon and reagent-grade NaF powder in a graphite crucible. Metallurgical-grade silicon was deliberately selected to introduce accurately measurable quantities of several impurities.

After cooling, samples of the two separate phases were analyzed by emission spectroscopy and the results are shown in Table 3. The distribution coefficient, $k_{(i)}$, for each impurity was determined from this rather crude melting experiment by comparing the concentration of impurity in sodium fluoride and silicon

$$k_{(i)} = \frac{C_{(i)} \text{ in NaF}}{C_{(i)} \text{ in Si}} \qquad (5)$$

It was assumed that impurity equilibrium was obtained while both phases were molten and that this impurity distribution was not altered on cooling. These distribution coefficients are also shown in Table 3. Large distribution coefficients are desirable to maximize transfer of impurities to the molten NaF phase. These results indicate that the melt separation of silicon will provide some additional purification of silicon because significant amounts of many impurities will accumulate in NaF.

If one assumes that impurities present in the reactants are accumulated in the silicon product during sodium reduction, then the redistribution of each impurity between the two reaction product phases on melting can be expressed as

$$C_o M_{Si} = C_{\ell} M_{Si} + k_i C_{\ell} M_{NaF} \qquad (6)$$

where C_o = Impurities in silicon before melting (all impurities are initially assigned to silicon arbitrarily.

C_ℓ = Impurities in silicon after melting

k_i = Impurities in NaF/impurities in Si on mutual melting and equilibration

M_{Si} = Mass of Si

M_{NaF} = Mass of NaF

The mass ratio, M_{NaF}/M_{Si}, of the reaction products of the SiF_4-Na reaction, carried out stoichiometrically, is

$$\frac{4NaF}{Si} = \frac{168}{28} = 6 \qquad (7)$$

The purification ratio, C_ℓ/C_o, is a measure of the extent of purification of liquid silicon resulting from impurity collection in NaF. From equations (6) and (7), the purification ratio C_ℓ/C_o is

$$\frac{C_\ell}{C_o} = \frac{1}{1 + 6k_i} \qquad (8)$$

Using the preliminary experimental distribution coefficients, k_i, shown in Table 3, we can calculate expected purification ratios; these are shown in Figure 11 as a plot of Equation (8), purification ratio versus distribution coefficient. Note that significant purification can occur even with modest values of the impurity distribution coefficients, and that melting the reaction products should purify the silicon of Al and Ca by two orders of magnitude and of Ni by one order of magnitude.

We are currently designing experiments to collect more accurate data on the impurity distribution coefficients involved in mutually melting NaF

Table 3

EMISSION SPECTROGRAPHIC ANALYSIS OF IMPURITIES IN Si AND NaF PHASES OBTAINED AFTER MELTING METALLURGICAL-GRADE SILICON WITH REAGENT-GRADE NaF IN A GRAPHITE CRUCIBLE
(ppm by weight)

Element	Metallurgical-Grade Silicon melted with Reagent-Grade NaF	NaF melted with Metallurgical-Grade Silicon	NaF Reagent Grade Blank	$k_i = \frac{C_{NaF}}{C_{Si}}$
Ti	600	90	< 6	0.15
V	200	50	< 5	0.25
Cr	125	35	< 3.5	0.28
Ni	60	80	< 8	1.33
Fe	2200	1000	< 7	0.45
Mn	300	25	< 4	0.08
Al	5	350	< 2.5	70.0
Ca	7	70	10.0	10.0
Cu	15	6	< 4.0	0.4

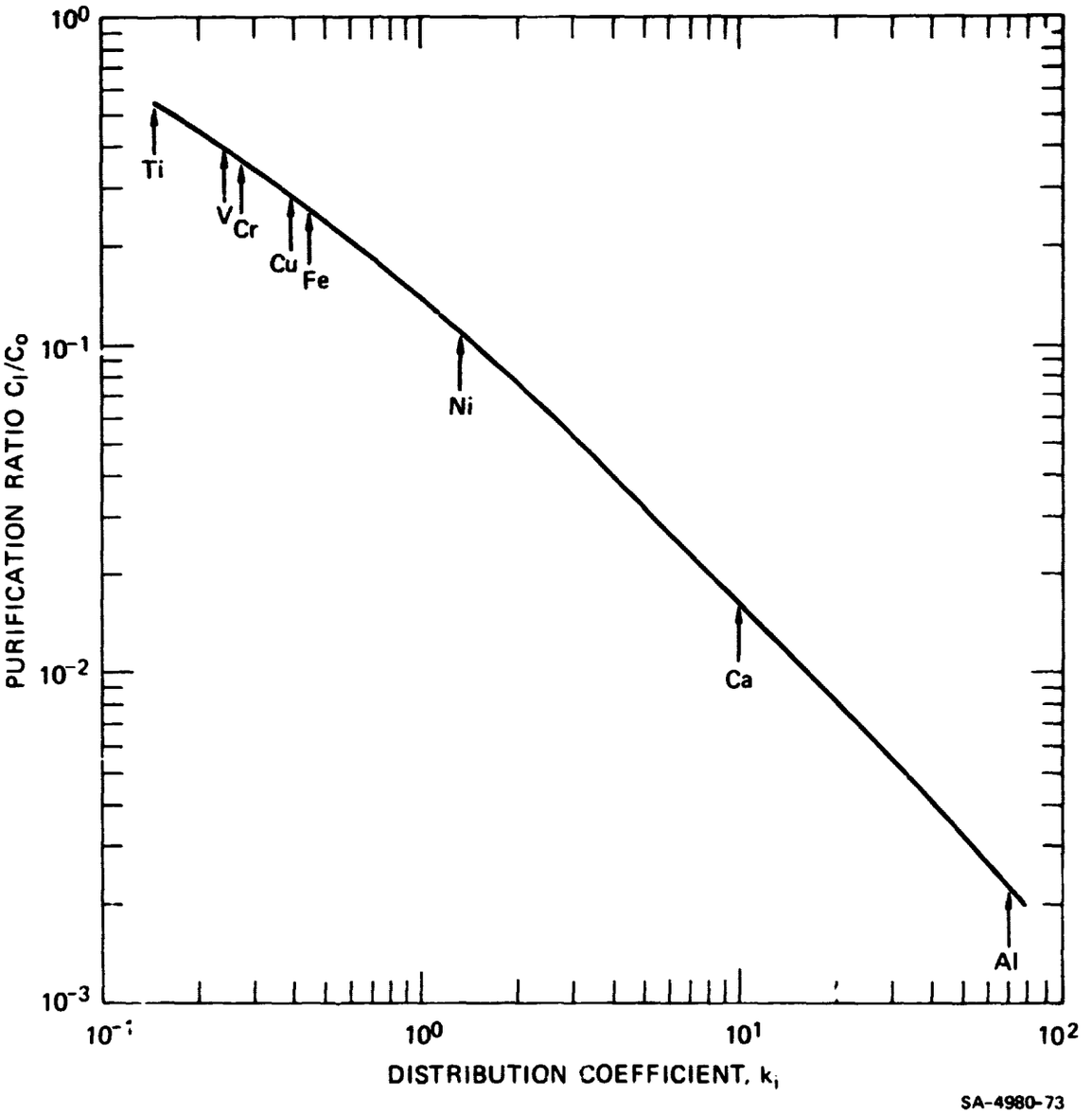


FIGURE 11 EXTRACTION OF IMPURITIES BY MOLTEN NaF IN CONTACT WITH MOLTEN Si

and Si. We will also determine the effect of a slight excess of SiF_4 (g) in the melt, which should shift by mass action the transfer of elements that are strong fluoride formers from silicon to NaF. This may increase the distribution coefficient, k_i, particularly for Ti, Zr and V. This would be consistant with Rhein's[4] findings that a slight stoichiometric excess of SiF_4 over Na is conducive to purification of some elements by conversion to their fluoride.

During these melt separation experiments, we observed that when solid chunks of metallurgical-grade silicon mixed with NaF were heated above 1410°C, under flowing Ar at >1.0 atm, a layer of brown powder deposited on the inner wall of the water-cooled quartz jacket around the crucible. X-ray diffraction of this brown fume revealed that it was a mixture of NaF and silicon. We believe that silicon transport takes place by the formation of SiF_2, SiF_3, and SiF_4 gases, which are formed at the melting point of silicon by the reaction of NaF with silicon. Thermodynamics calculations for the system Si + NaF + Ar gas, performed by Rhein,[5] indicate the equilibrium concentrations of various components in the gas phase as shown in Figure 12. Silicon could be transported by any of the following three mechanisms:

$$2\,SiF_2\,(g) \rightarrow Si + SiF_4 \qquad (9)$$

$$\begin{aligned} 2\,SiF_3\,(g) &\rightarrow Si_2F_6(g) \\ Si_2F_6 &\rightarrow SiF_2(g) + SiF_4(g) \\ 2\,SiF_2\,(g) &\rightarrow Si + SiF_4(g) \end{aligned} \qquad (10)$$

$$\begin{aligned} SiF_4(g) + Si(melt) &\rightarrow 2\,SiF_2(g) \\ 2\,SiF_2(g) &\rightarrow Si + SiF_4(g) \end{aligned} \qquad (11)$$

[4] Robert Rhein, Jet Propulsion Laboratory, private communication, November 1978.

[5] Robert Rhein, ibid., July, 1978.

ORIGINAL PAGE IS
OF POOR QUALITY

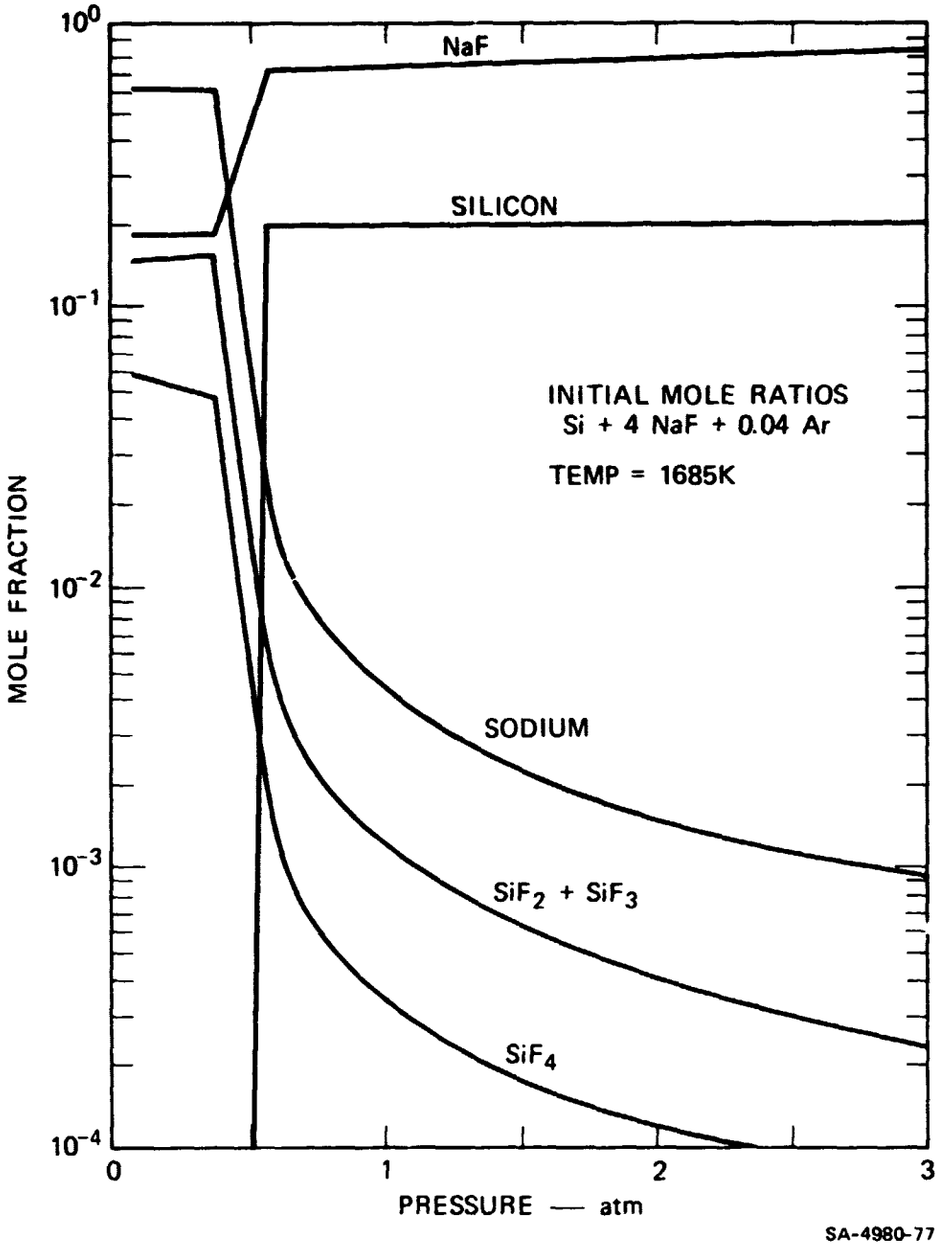


FIGURE 12 CALCULATED CHANGE IN THE EQUILIBRIUM MOLE FRACTION OF VARIOUS COMPONENTS IN THE GAS PHASE OF THE Si-NaF-Ar SYSTEM WITH TOTAL PRESSURE

Purification of Silicon by Solidification

Purification of silicon by impurity transfer to NaF(ℓ) during melting can be followed by further purification during solidification of the molten silicon. These phenomena are cumulative in their effect on the final impurity distribution in the solid silicon.

Boron and phosphorous concentrations in silicon produced by sodium reduction of SiF_4 or Na_2SiF_6 usually range from 100 to 200 parts per billion by weight. Metal impurity concentrations range up to a few parts per million by weight. Table 4 shows the results of a Spark Source Mass Spectrometric analysis (SSMS) of a typical batch of SRI silicon before melting. (Purity has been improved in our recent experiments for solid sodium feeding in the SiF_4-Na reaction, as described in Section 1.)

Silicon can be further refined after melting by either of two techniques: Czochralski crystal growth or slow directional solidification. For a well mixed residual liquid phase during solidification, the segregation of impurities between the solid and liquid silicon phases takes place according to

$$C_s = C_\ell K_o (1 - g)^{(K_o - 1)} \tag{12}$$

where

C_s = Impurity concentration (atoms cm^{-3} in solid phase)

C_ℓ = Impurity concentration (atoms cm^{-3} in the starting material)

K_o = Solid/liquid segregation coefficient for an impurity in silicon

g = Fraction of the material solidified ($g = V_s/V_\ell$).

For very low segregation coefficients ($K_o < 1$), equation (12) reduces to

$$C_s = \frac{C_\ell K_o}{1-g} \tag{13}$$

Table 4

IMPURITY ANALYSIS OF SILICON BY SSMS

Element	ppm by weight	Atoms $cm^{-3} \times 10^{-16}$
B	0.1	1.3
Al	0.8	4.2
P	0.2	0.9
Ti	2.0	5.8
V	0.04	0.1
Zr	2.0	3.0
Mo	0.3	0.4
Cr	12.0	32.3
Mn	0.1	0.3
Fe	55.0	137.8
Cu	22.0	48.5
Ni	2.0	4.8
Mg	0.1	0.6
Ca	1.0	3.5
Na	1.0	6.0
F	0.1	0.7

Using equations (12) and (13) and the SSMS values in Table 4 for C_s, we calculated impurity concentrations in the solid phase (C_s) for different values of g in the range of 0.5 to 0.9. The segregation coefficients used in these calculations for various impurities are given in Table 5. These values of C_s for various impurity elements in the silicon obtained by the SiF_4-Na reaction are plotted against g (the fraction of solidified material) in Figure 13. In these calculations equation (12) was used for boron and phosphorous because their K_o values, 0.8 and 0.35, respectively, are comparable to 1, whereas equation (13) was used for the rest of the impurities because $K_o \ll 1$. It was assumed that segregation of any single impurity between the solid and liquid phases was independent of the presence of the other impurities in silicon.

Table 6 shows the permissible level for various impurities in silicon for solar cells, both for n- and p-type silicon, according to R. H. Hopkins, et al.[6]

Table 5

SEGREGATION COEFFICIENTS FOR VARIOUS IMPURITIES

Element	Segregation Coefficient
Al	2.8×10^{-3}
B	0.8
Cu	8.0×10^{-4}
Cr	1.1×10^{-5}
Fe	6.4×10^{-6}
Mg	3.2×10^{-6}
Mn	1.3×10^{-5}
Mo	4.5×10^{-8}
Ni	3.2×10^{-5}
P	0.35
Ti	3.6×10^{-6}
V	4×10^{-6}
Zr	1.6×10^{-8}

[6] R. H. Hopkins, et al., "Silicon Materials Task of the Low Cost Silicon Array Project (Phase II)," Quarterly Report No. 10, DOE/JPL-954331-78/2 (1978).

Table 6

PERMISSIBLE IMPURITY CONCENTRATIONS IN SOLAR CELL SILICON*

Element	Permissible Level, Atoms cm^{-3}	
	n-type Si	p-type Si
Cu	10^{15}	10^{15}
Aℓ	10^{15}	--
Ni	6×10^{13}	5×10^{14}
Fe, Cr, Mn	2×10^{14}	3×10^{13}
Ti	10^{13}	10^{12}
Zr	10^{12}	10^{11}
V	10^{13}	10^{11}

*Reference 5.

ORIGINAL PAGE IS
OF POOR QUALITY

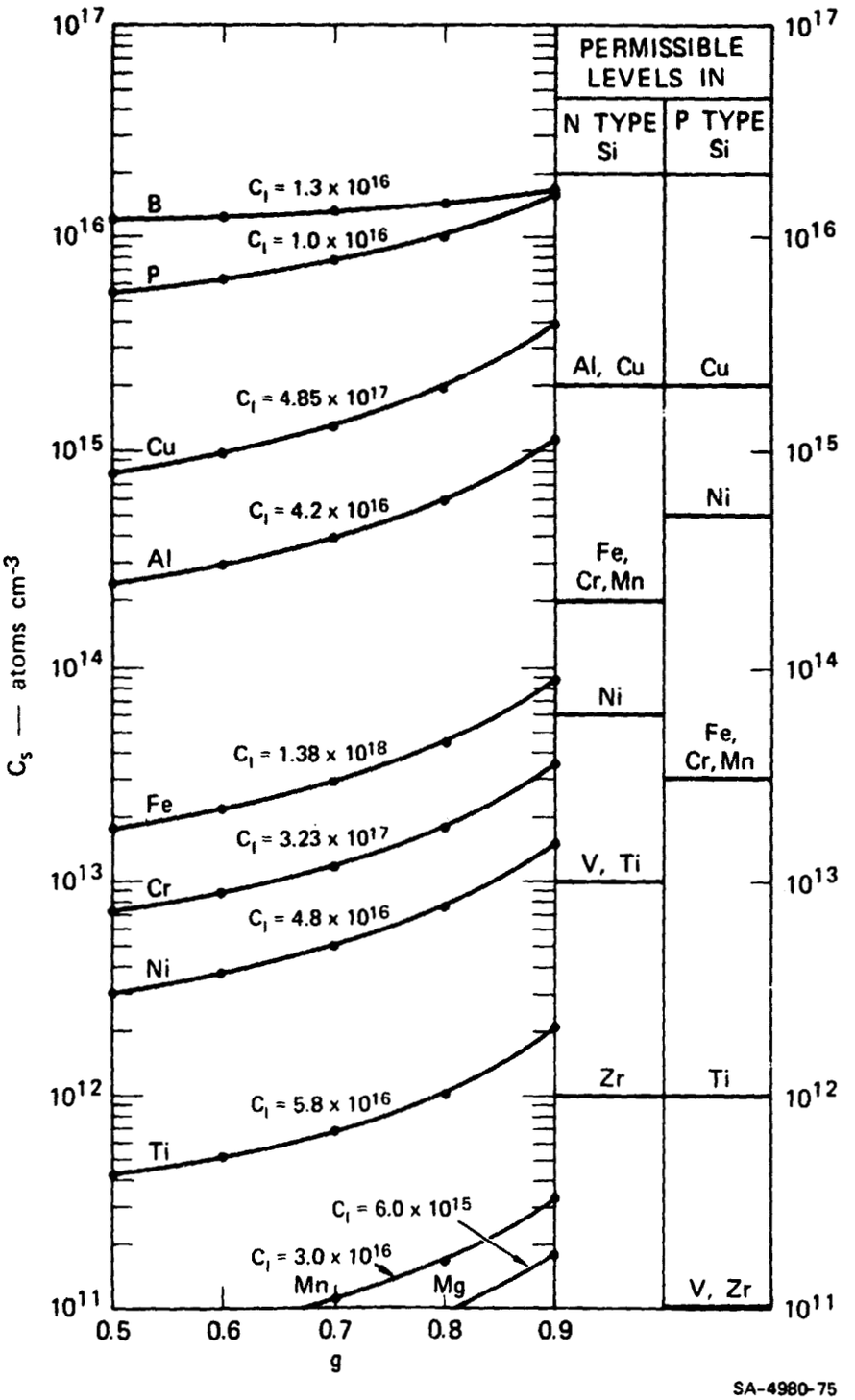


FIGURE 13 SILICON PURIFICATION BY DIRECTIONAL SOLIDIFICATION

For comparative purposes, Figure 13 shows the permissible concentrations both for n- and p-type silicon.

It is clear that for the n-type silicon base, the impurity level for most of the elements except Cu remains below the maximum permissible level, even after 90% of the melted silicon is solidified. However, for a p-type silicon base, the maximum permissible level is just exceeded for Cu and Ti at 80% solidification and for Fe at 70% solidification. The concentrations of Zr, V, and Mo in the solid drop below 10^{11} atoms cm^{-3}. However, copper and iron concentrations in the starting silicon, C_{ℓ}, have been substantially lowered in subsequent sodium reduction experiments. No significant improvement in the concentrations of B and P in the solid phase was expected from unidirectional solidification. However, these impurity concentrations are acceptably low to start with in silicon produced by sodium reduction of SiF_4.

Thus, it appears that the silicon produced by the SiF_4-Na reaction could be adequately purified by batch melting and solidification of 90% of the melt to meet solar-grade specifications. This conclusion ignores further purification resulting from impurity transfer to molten NaF.

To improve and scale-up Si/NaF melting experiments, a used furnace for silicon crystal growth has been purchased and assembled and is being modified for melting experiments. This furnace has a 7 in. high by 8 in. deep graphite heating element and it can accommodate 5 in. ID crucibles. Larger quantities of the reaction product mixture obtained from sodium reduction of SiF_4 or Na_2SiF_6 will be melted and separated by gravity as immiscible liquid phases in this furnace. This apparatus can also serve as a high temperature sodium reduction reactor using Na (ℓ) and SiF_4(g), or Na(ℓ) and Na_2SiF_6, proceeding to melting and separation of the product phases in the same vessel.

The furnace power system and temperature controller have been assembled. However, during initial operational checkout a crack was detected in the water-cooled furnace reactor shell; the crack has been removed from the furnace and is now being repaired. A new heating element and other graphite parts have been delivered.

We also plan to do reaction product (Si-NaF) melt experiments in air using a SiC crucible. Once the NaF is melted it may be able to protect Si from significant oxidation.